First-principles study of the stability and edge stress of nitrogen-decorated graphene nanoribbons

Yierpan Aierken,[*] Ortwin Leenaerts,[†] and François M. Peeters[‡]
Department of Physics, University of Antwerp, Groenenborgerlaan 171, 2020 Antwerpen, Belgium

(Received 9 May 2018; published 25 June 2018)

Edge functionalization of graphene nanoribbons with nitrogen atoms for various adatom configurations at armchair and zigzag edges are investigated. We provide comprehensive information on the electronic and magnetic properties and investigate the stability of the various systems. Two types of rippling of the nanoribbons, namely edge and bulk rippling depending on the sign of edge stress induced at the edge, are found. They are found to play the decisive role for the stability of the structures. We also propose a type of edge decoration in which every third nitrogen adatom at the zigzag edges is replaced by an oxygen atom. In this way, the electron count is compatible with a full aromatic structure, leading to additional stability and a disappearance of magnetism that is usually associated with zigzag nanoribbons.

DOI: 10.1103/PhysRevB.97.235436

I. INTRODUCTION

Graphene nanoribbons (GNR) consist of strips of graphene sheets having nanoscale width, while along the strip the GNR extends to macroscopic dimensions. It is important for applications that the electronic properties can be tuned. There are four main approaches to achieve this for such GNRs. First of all, the band gap of a GNR is inversely proportional to its width due to quantum confinement effects [1,2], so that narrow GNRs have larger band gaps. Second, the type of edge of the GNR can influence its properties. For example, an armchair-edged GNR (AGNR) has non-spin-polarized edges whereas a zigzag-edged GNR (ZGNR) is magnetic. More precisely, the magnetic ground state of the zigzag edges has ferromagnetic ordering along each edge and antiferromagnetic ordering across the edges. Third, an external electric or magnetic field also changes the properties of the GNR [3–6]. Here, we tune the GNR properties through edge decoration with adatoms. We use the notation X-GNR throughout the paper to represent a GNR decorated by element X.

Chemical functionalization of the unsaturated edges can have a huge impact on the properties of GNRs. Wang *et al*. [7] reviewed different types of methods to synthesize heteroatom-doped graphene materials and the resulting material properties and applications, and emphasized on the experimental accessibility. Gorjizadeh and Kawazoe [8] reviewed some of the early studies on chemical functionalization of GNR edges. The possibility to induce different magnetic ground states from half-metallic to half-semiconducting was reported. These different electronic states are realized by only changing the elements at the GNR edge. Lee and Cho [9] studied ZGNRs with several organic compounds adsorbed at the edges, while Huang *et al*. [10] reported possible induction of spiral magnetic order through transition-metal atomic chain decoration. Another study [11] suggests the possibility of achieving a half-metallic GNR by doping different species at different edges. Chang *et al*. [12] investigated curved GNRs to simulate unzipping of graphene nanotubes through edge decoration with elements whose atomic number is less than 30. Cervantes-Sodi *et al*. [13] reported detailed studies on the electronic and magnetic properties of edge-decorated GNR with H, N, and O atoms. They discovered that single edge decoration of a ZGNR can give a half-semiconductor band gap, and the properties of the system vary significantly with the type of atoms attached to it. Several promising synthesis methods have been studied to show the accessibility of GNRs using different approaches [14–17]. From unzipping of nanotubes to bottom-up approaches, atomic precision on the structure of the GNR can be realized down to 1 nm with smooth edge structures. Lin *et al*. [18] investigated functionalization with edge adatoms whose atomic number is less than 20 as edge adatoms for AGNRs. They aimed to list the most stable configuration for each element from a total energy perspective. Among these elements, they concluded that nitrogen atoms have the largest binding energy and thus form the most stable adatom. Besides this, N atoms have an atomic radius comparable to that of C, so that they do not distort the GNR structure significantly. The five electrons in nitrogen were shown to reduce the chemical reactivity of the GNR edges. Wang *et al*. [19] studied the possibility of such a process experimentally and reported how this can be used to tune the electronic properties of the GNR. Several other studies [20–22] have drawn the conclusion that doping at the edges of a GNR is generally favored, by 0.5 eV/N atom, as compared to bulk doping at the interior part of the GNR.

Despite this large collection of literature on N-GNR, a systematic study about its most stable configurations on both zigzag and armchair edges without H saturation is still missing. Here the edge functionalization involves both edge doping and adsorption at the edge. This paper aims to fill this gap and studies the electronic and magnetic properties of four stable N-GNRs and their dependence on the GNR's width using first-principles calculations. Special attention is given to the

[*]yierpan.aierken@uantwerpen.be
[†]ortwin.leenaerts@uantwerpen.be
[‡]francois.peeters@uantwerpen.be

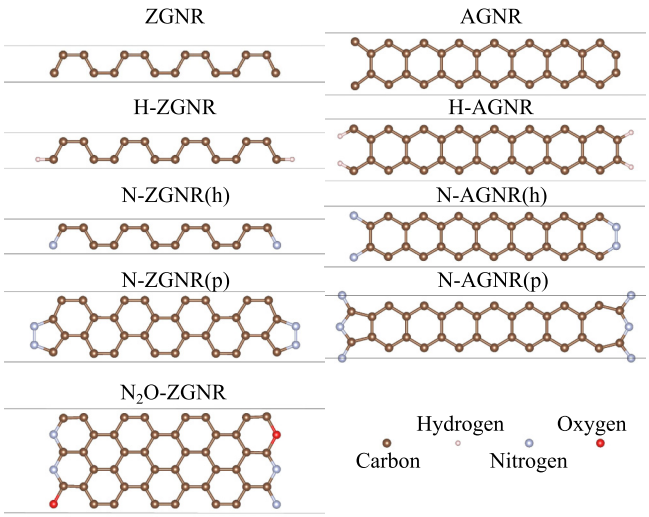

FIG. 1. Structure of the edge-decorated and pure GNRs considered in this paper.

study of the edge stability. We predict structural distortions that stabilize the N-decorated edge systems by applying perturbations to the unstable flat structures according to their imaginary phonon modes or by performing *ab initio* molecular dynamics calculations at finite temperature. We quantify the nature of these distortions by calculating the edge stress and show their relationship.

Four possible edge structures are proposed for the N-GNRs, namely N-AGNR(h), N-AGNR(p), N-ZGNR(h), and N-ZGNR(p). Their structures are shown in Fig. 1. The *h* and *p* labels denote if the structure has pentagonal or hexagonal edge structures, respectively. These edges have been observed experimentally [23]. For example, edge nitrogen adsorption can form a five-membered (pyrrolic) ring on the edge of a ZGNR or a six-membered ring (pyridinic) on the edge of an AGNR, and they are corresponding to peaks at 400 eV and 398 eV in XPS spectra [23,23–25], respectively. The calculated formation energies of these types of edges with a single adsorbed N_2 molecule in Jeon *et al.* [23]'s paper are $-2.5\,\mathrm{eV}/N_2$ for the N-ZGNR(p) and $1.96\,\mathrm{eV}/N_2$ for the N-AGNR(h). These results are in good agreement with our results, i.e., $-2.75\,\mathrm{eV}/N_2$for the N-ZGNR(p) and $2.05\,\mathrm{eV}/N_2$ for the N-AGNR(h). The N-GNR(type I) in Lin *et al.* [18]'s paper is the same structure as our N-AGNR(p). Our results for the electronic structure and the adsorption energy of N are consistent with theirs. However, as will be discussed in the results section, a planar form of this structure is not stable as indicated by the presence of imaginary frequencies in the phonon spectrum. Instead, a long wavelength distortion along the nanoribbon is preferred. Such instabilities are not just limited to N-AGNR(p), but apply to other structures as well. Nevertheless, as the structure remains quite smooth locally, the electronic properties are not significantly influenced by the distortion. In addition, we also propose a structure by replacing every third N atom in N-ZGNR(h) with oxygen to have a semiconductor with a larger band gap due to a more balanced electron count. This structure is denoted as N_2O-ZGNR in the text. The electronic stability is enhanced by making the edge aromatic compatible, such that, as we will see, its energetic stability is as good as that for H-GNR.

II. COMPUTATIONAL DETAILS

Here we first list all the details on the first-principles calculations:

(i) Theoretical methodology: density functional theory

(ii) Simulation package: Vienna *ab initio* simulation package (VASP) [26–29]

(iii) Basis set: plane-wave (500 eV energy cutoff)

(iv) Exchange-correlation functional: Perdew-Burke-Ernzerhof (PBE-GGA) [30,31]

(v) k points: $1 \times 1 \times 25$

(vi) Energy convergence (electronic step): 10^{-5} eV

(vii) Force convergence (ionic step): 10^{-3} eV/Å

(viii) Phonon calculation method: finite displacement method

(ix) Phonon calculation supercell: GNR with 20 Å length

(x) *Ab initio* molecular dynamics: Parrinello-Rahman (NpT) dynamics [32,33] with a Langevin thermostat at 100 K with 2 fs time steps for a total simulation time of 6 ps

The edge stress calculations follow the same method as described in Ref. [34]. The boundary stress γ is expressed in terms of the boundary energy σ and its first derivative with respect to strain e as follows:

$$\gamma = \sigma + d\sigma/de. \tag{1}$$

The boundary energy σ is defined as follows:

$$\sigma = (E_t - N_C E_g - N_X E_X)/2L, \tag{2}$$

where E_t is the total energy, E_g is the energy per atom of graphene, N_C and N_X are the number of C atoms and X adatoms in the nanoribbon, E_X is the total energy per X atom in its stable molecular form, i.e., H_2, N_2, and O_2. L is the lattice constant along the nanoribbon. Two values for the strain along the nanoribbon axis, e, were considered, namely 0.5% and 1.0%.

III. RESULTS

A. Energetic stability

Let us first consider the energy aspects of the different N-GNR structures shown in Fig. 1 as a function of their width. For this, we let the width vary from approximately 5 to 25 Å. For comparison, we also show the results for unsaturated bare ribbons, denoted as GNR, and H-decorated GNR, denoted as H-GNR. Hereafter, we make use of three different energies, namely the formation, adsorption, and boundary energy. The formation energy, E_f, is defined as the difference between the energy of the total system (GNR with edge atoms) and the sum of the energies of the isolated elemental systems (i.e., graphene, N_2, H_2, and O_2), divided by the total number of atoms in the system. This energy determines the energetic stability of the GNR system with respect to its parent components before forming the GNR system. The adsorption energy, E_a, on the other hand, is defined as the difference in energy of the X-GNR system and the sum of the energy of a bare GNR of the same width and the relevant X molecular energies. The adsorption energy indicates whether adatoms X will adsorb

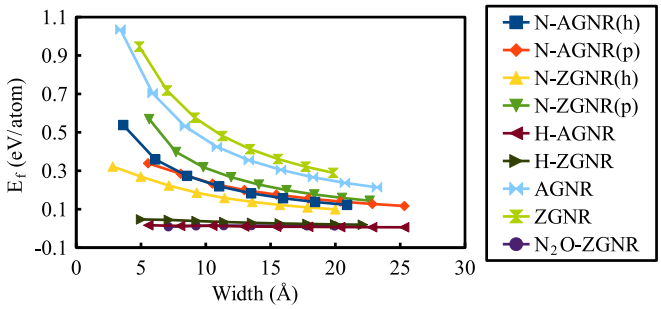

FIG. 2. Formation energies E_f as a function of the width of the GNR for different edge atoms.

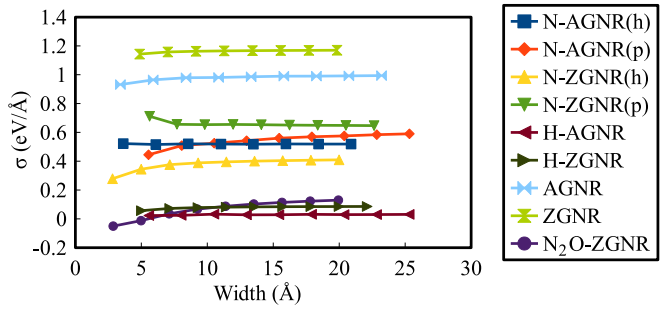

FIG. 4. Boundary energies σ as a function of the width of the GNR for different edge atoms.

on a preformed graphene edge. The boundary energy, which was defined in the previous section, gives an indication of how easily an edge in a graphene sheet can be created in a molecular atmosphere.

Results of the formation energy per atom are shown in Fig. 2. As expected, the formation energy per atom decreases with increasing GNR width because the relative amount of edge atoms decreases with increasing width. All formation energies are positive, so none of the systems is spontaneously formed at low temperature. However, the formation energies of the H-GNR and N_2O-ZGNRs are very low and these structures should be relatively easy to be made under suitable circumstances [35]. Note that the formation energy of H-GNRs and N_2O-ZGNRs is approximately constant as a function of GNR width, indicating that these edges are quite stable. This will be discussed in more detail below.

When a GNR is created and subsequently brought into contact with possible adatoms, it is the adsorption energy that determines whether the reaction can proceed. The adsorption energy of the differently decorated GNR systems is shown in Fig. 3. Lee and Cho [9] found the binding energy for a single H atom to a bare ZGNR edge is 5.73 eV/H atom when using a local spin density approximation (LSDA) functional, while we have 4.95 eV/H atom using a GGA functional. Since overbinding is a common feature of the former functional [36], the agreement is reasonable. Since these energies are all negative, these decorated GNR systems can in principle be made if a good reaction pathway is found. The adsorption energy is also almost independent of the GNR width, which shows that the adatom adsorption is a local process. It is seen that all adatoms prefer the zigzag edges. The fact that the H

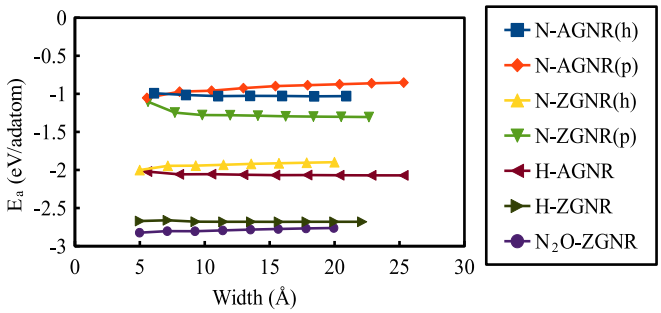

FIG. 3. Adsorption energies E_a as a function of the width of the GNR for different edge atoms.

atoms have lower adsorption energies than N atoms results mainly from the higher binding energy in a N_2 molecule as compared to H_2. Interestingly, the N_2O decoration has the lowest adsorption energy. To explain this result, one should take into account the electron count of the system. According to Clar's theory for GNRs, the benzoid rings become broken at zigzag edges. As demonstrated by Wassmann *et al.* [35], the introduction of adatoms at the edges of such nonbenzenoid ribbons can restore the Clar sextets in the system. With hydrogen, this can be done by introducing one extra H atom at every third edge atom in a H-GNR. In a N-ZGNR, the Clar sextets can be restored by substituting every third N adatom with an O atom which contains one extra electron. In this way, the electron count is compatible with a full aromatic structure, leading to increased stability.

The last important energy that we consider is the boundary energy. This energy is the same as the formation energy but it is defined per unit length of GNR edge and is shown in Fig. 4 for different widths. Its importance lies in the process of calculating edge stress later on. Nevertheless, we compared the results for bare GNR and our results are consistent with previous calculations [37]. Similar to the formation energy, we can also conclude from this figure that H atoms and the combination of N and O atoms near a graphene surface will enhance edge formation considerably. As for the adsorption energy, we find that the boundary energy is almost independent of the GNR width. This also means that the creation of an edge doesn't depend on the presence of other edges in the system. Edge formation is therefore also a local process.

B. Electronic structure

After establishing the energetic stability of the edge-decorated GNRs, it is worthwhile to briefly cover some of the important features of their electronic structure before we present the results on their dynamical stability. The band structures are shown in Fig. 5. Both AGNR and ZGNR without edge decoration are semiconductors in the whole range of width considered, as shown in Fig. 6. The band extrema of AGNRs with or without H are located at the Γ k point, while they are located between the Γ and X k points for zigzag ones. Although the band gaps decrease overall with increasing width of GNR, the band gaps of the AGNRs can be divided into three families which show an offset with respect to each other, see Fig. 6. This behavior can be theoretically explained by the different symmetries of the corresponding systems [38].

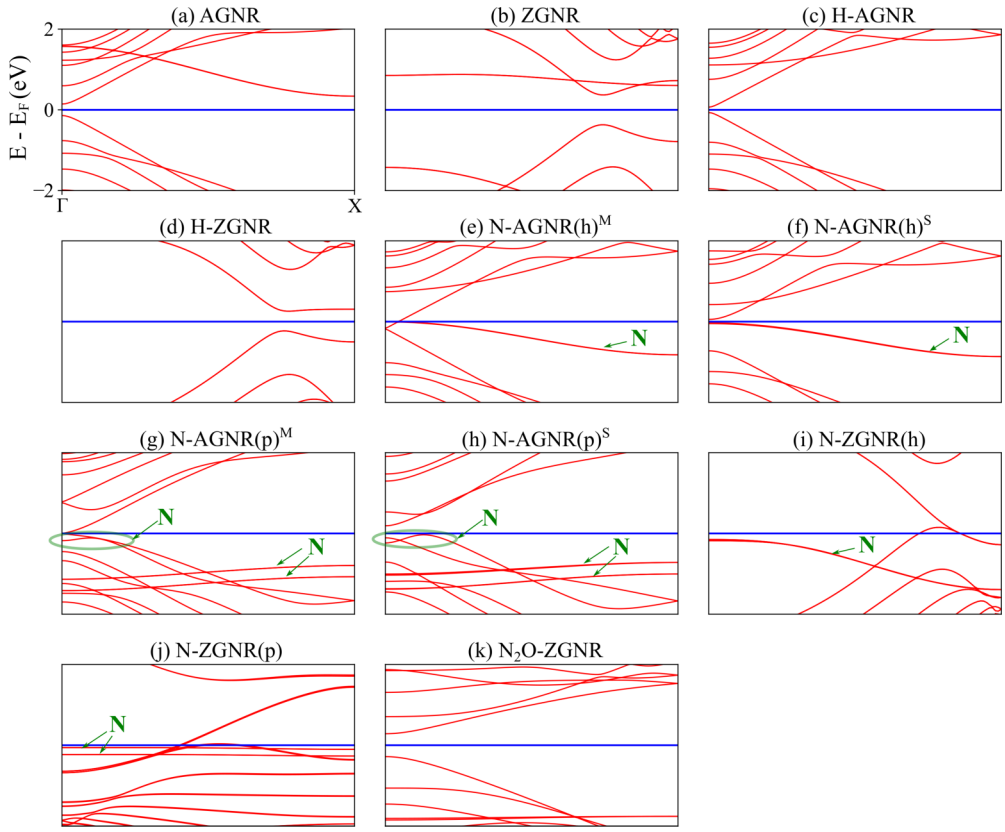

FIG. 5. Band structure of edge-decorated and pure GNRs. Superscripts indicate whether the system is metallic (M) or semiconducting (S) for N-AGNR(h) and N-AGNR(p). Bands associated with N atoms are marked with green arrows. The Fermi energy E_F, marked by a horizontal blue line, is inside the band gap for semiconductors. All the subfigures share the same axis and tick label as in the first one.

When the GNRs are decorated with N atoms, three of the five N valence electrons participate in bonding with C atoms, while the other two form a free electron pair that is localized on the N atoms. These localized states are seen as the less dispersive bands in Fig. 5. Their top defines the Fermi level in N-AGNR(h). Apart from these localized states, the overall band structure of N-AGNR(h) is similar to H-AGNR. This is expected because the N atom has a similar atomic radius as the C atoms and is mainly different from C by the extra electron it has. This extra electron saturates the dangling bond that a C atom would have at the edge, while for H-GNR, the dangling bond is removed by the bond with H. This situation is no longer true when pentagons are introduced, i.e., N-AGNR(p). First of all, the localized bands are still present but the degeneracy of the bands coming from two N atoms at the same edge in a unit cell is now lifted since these two atoms are no longer equivalent. Their energies are also lowered with respect to the Fermi energy as compared to the N-AGNR(h) case. Furthermore, here only a small section of the bands in the gap are associated with N atoms as marked by ellipses in Figs. 5(g) and 5(h). This part gives a nonbonding character thus a higher energy compared to the rest of the band which associates with C atoms and involves π bonds. The other band structures are similar as for H-GNR. For example, for the armchair structures, the three families of band gaps are also present in N-AGNR, but the smallest band gap family is now metallic, see Fig. 7.

The magnetic ground states of all systems were checked. All armchair GNRs with or without edge decoration are nonmagnetic. The zigzag GNRs, on the other hand, are

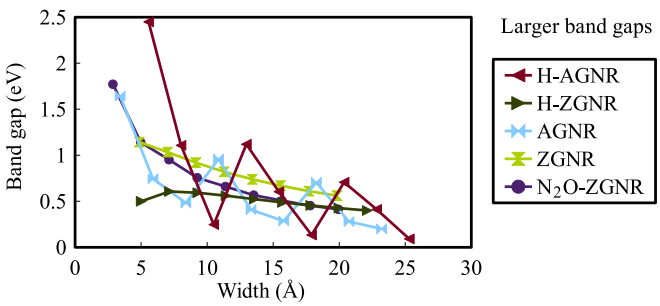

FIG. 6. Band gaps of edge-decorated and pure GNRs as a function of their width.

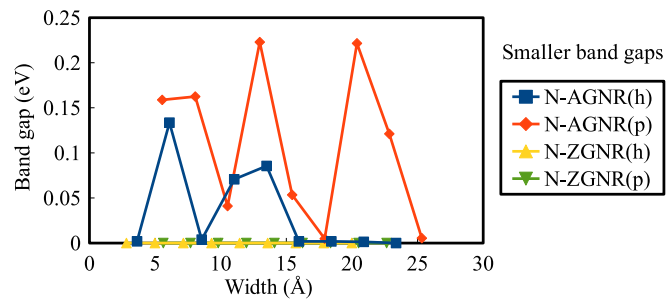

FIG. 7. Band gaps of N-GNRs as a function of their width.

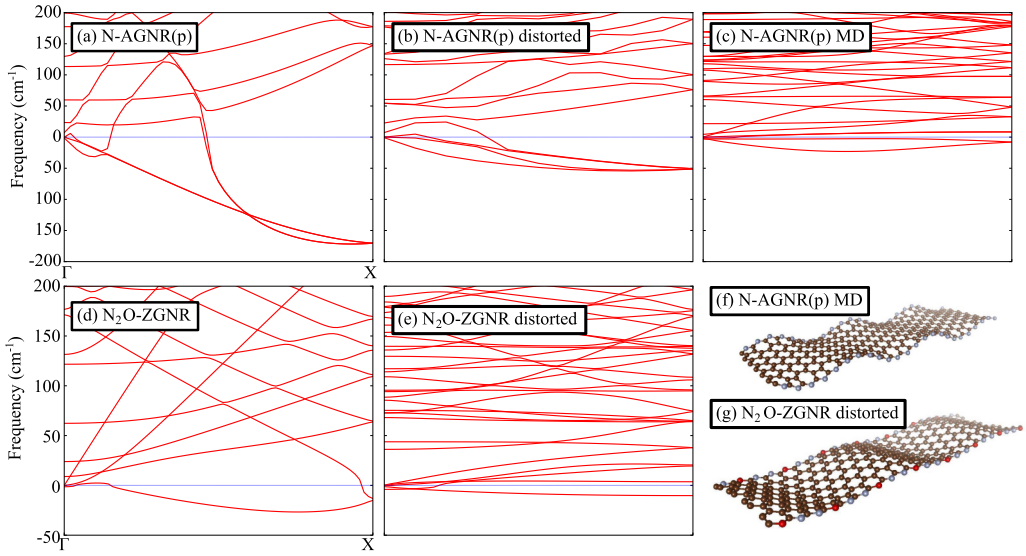

FIG. 8. (a)∼(e) are the phonon dispersion evolutions as the structures are distorted manually or via MD at finite temperature. (f) and (g) are the final structures of N-AGNR(p) and N_2O-ZGNR, respectively.

ferromagnetic along the edge and antiferromagnetic across the ribbon. The former lowers the total energy by introducing exchange splitting for the π band, whereas the latter makes sure the magnetic tails from the two edges interact constructively inside the GNR, increasing the exchange splitting [39]. We also observed less than 1 meV/atom lowering in total energy if the N-ZGNR were ferromagnetically ordered across the ribbon. The magnitude of magnetization is reduced in the following order: ZNGR, H-ZGNR, and N-ZGNR. Due to the full aromatic nature of the N_2O-GNR, no magnetism is observed in that case.

C. Dynamical stability and edge stress

Here we investigate the dynamical stability of all the N-GNRs. The dynamical stability is checked by calculating the phonon spectra of the various systems. In Figs. 8(a) and 8(d), we show two typical phonon spectra, while those of the other systems are included in Fig. S1 in the Supplemental Material [40]. Note that, up to now, we assumed all structures to be flat. However, most spectra of these flat structures are seen to contain imaginary frequency modes, which indicates they are not dynamically stable. To find the origin of these instabilities, we followed two different approaches: One is to distort the structure according to the vibrational mode that gives the imaginary frequency and subsequent relaxation, leads to a more stable structure; the other one is to perform a finite-temperature *ab initio* molecular dynamics simulation where thermal fluctuations distort the structure and lead to a lower free energy. Next, we performed phonon calculations on the resulting distorted structures. The evolution of the imaginary frequency as the structure is distorted is illustrated in Fig. 8. From both approaches, we found that either the edges or the interior of the edge-decorated GNRs show long wavelength ripples which stabilize the structure [see Figs. 8(f) and 8(g)]. The actual wavelength of these ripples is difficult to achieve with our methods which basically depend on the supercell size. Here, the computational cost to simulate a longer GNR having longer wavelength ripples is too high, especially the phonon calculations for a such distorted structure. The important feature that we want to point out here is the significant stability enhancement upon ripples induction. We believe the stable structure that has no imaginary phonon frequency would have a similar structure, but to determine the exact shape and length of the ripples is difficult.

To put these results on a more quantitative basis, we therefore calculated the boundary stress γ for the different ribbons, as shown in Table I. Positive values for the boundary stress γ indicate that the edge tends to occupy less space and therefore tries to reduce the length of the GNR, as in the case of N_2O-ZGNR. This results in interior rippling of the GNR. Negative γ values, on the other hand, indicate that the edge tends to expand and causes a rippled edge, as in the case of N-AGNR(p). It is interesting to note that the magnitude of the boundary stress is related to the degree of instability. For example, N-AGNR(p) has a larger absolute value of boundary stress and consistently more negative phonon frequencies than those of N_2O-ZGNR, see Table I and Figs. 8(a) and 8(d).

TABLE I. Boundary energy σ and edge stress γ of N-GNRs and the reference systems.

Type	Boundary energy σ eV/Å	Stress γ eV/Å
AGNR	1.01	− 2.21
ZGNR	1.18	− 1.07
H-AGNR	0.03	− 1.35
H-ZGNR	0.09	− 0.51
N-AGNR(h)	0.52	0.88
N-AGNR(p)	0.67	− 6.04
N-ZGNR(h)	0.43	3.30
N-ZGNR(p)	0.65	0.63
N_2O-ZGNR	0.06	2.81

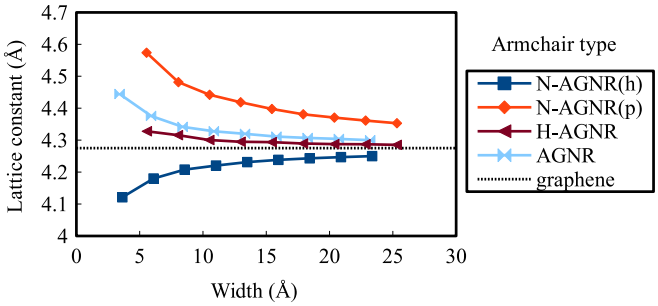

FIG. 9. The lattice constants along the AGNRs as a function of their widths. The value for graphene is given for the reference.

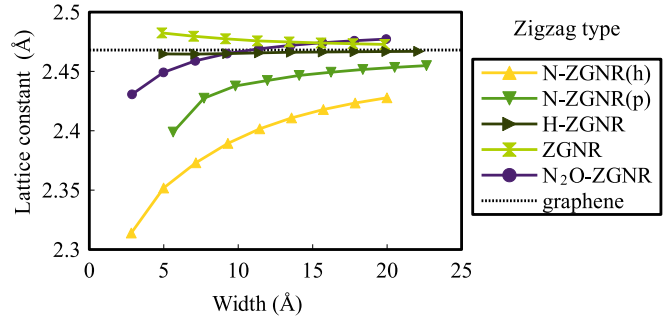

FIG. 10. The lattice constants along the ZGNRs as a function of their widths. The value for graphene is given for the reference.

Similar conclusions can be reached by considering the lattice constants of all GNRs against their width, see Fig. 9 and Fig. 10. For flat structures, we clearly observe a convergence of the lattice constant towards that of graphene as the width increases. However, some structures are increasing while the others are decreasing their lattice constants. If we compare this to Table I, we see that these two groups have opposite sign for their stress values in the table. To accommodate the negative stress value, which corresponds to the edge's tendency for expansion, the GNR increases its lattice constant. However, this becomes expensive as the width of the GNR increases. Such a picture is very useful to see what type of stress and distortion can be expected when making such edge-decorated GNRs at different widths.

IV. SUMMARY

This work fills the void left by the absence of a systematic study on N adsorption and substitutional doping at the edge of GNR without H saturation. Together with our newly proposed N_2O-GNR structure, i.e., a N-decorated ZGNR structure with every third N replaced by O along the edge to balance the number of electrons, we listed all energetically favored configurations for N-decorated GNRs. A thorough study on the stability of these structures from different energy perspectives was presented and a description of their electronic structure was given. We discovered a dynamical instability of flat structures, even at low temperature, by calculating the phonon spectrum. In search for more stable structures, we either followed the phonon mode that gives an instability, or we performed *ab initio* molecular dynamics to perturb the structure. In this way, we revealed the formation of ripples either at the edge or at the interior of the GNR to stabilize the structure. To confirm this conclusion, we calculated the edge stress and linked its sign to the tendency of the edge to expand or shrink. Finally, we showed that these results are also consistent with the change in lattice constant along the ribbon length upon doping.

ACKNOWLEDGMENTS

This work was supported by the Fonds Wetenschappelijk Onderzoek (FWO-Vl). The computational resources and services used in this work were provided by the VSC (Flemish Supercomputer Center), funded by the Research Foundation - Flanders (FWO) and the Flemish Government - department EWI.

[1] Z. Chen, Y.-M. Lin, M. J. Rooks, and P. Avouris, Phys. E Low-dimensional Syst. Nanostructures **40**, 228 (2007).
[2] M. Y. Han, B. Özyilmaz, Y. Zhang, and P. Kim, Phys. Rev. Lett. **98**, 206805 (2007).
[3] S.-Q. Zhao, Y. Lü, W.-G. Lü, W.-J. Liang, and E.-G. Wang, Chin. Phys. B **23**, 067305 (2014).
[4] Y.-W. Son, M. L. Cohen, and S. G. Louie, Nature (London) **444**, 347 (2006).
[5] W. Y. Kim and K. S. Kim, Nat. Nano **3**, 408 (2008).
[6] J. Klinovaja and D. Loss, Phys. Rev. X **3**, 011008 (2013).
[7] X. Wang, G. Sun, P. Routh, D.-h. Kim, W. Huang, and P. Chen, Chem. Soc. Rev. **43**, 7067 (2014).
[8] N. Gorjizadeh and Y. Kawazoe, J. Nanomater. **2010**, 513501 (2010).
[9] G. Lee and K. Cho, Phys. Rev. B **79**, 165440 (2009).
[10] C. Huang, H. Wu, K. Deng, and E. Kan, J. Phys. Chem. C **121**, 1371 (2017).
[11] E.-j. Kan, Z. Li, J. Yang, and J. G. Hou, J. Am. Chem. Soc. **130**, 4224 (2008).
[12] S.-L. Chang, S.-Y. Lin, S.-K. Lin, C.-H. Lee, and M.-F. Lin, Sci. Rep. **4**, 6038 (2014).
[13] F. Cervantes-Sodi, G. Csányi, S. Piscanec, and A. C. Ferrari, Phys. Rev. B **77**, 165427 (2008).
[14] T. H. Vo, M. Shekhirev, D. A. Kunkel, M. D. Morton, E. Berglund, L. Kong, P. M. Wilson, P. A. Dowben, A. Enders, and A. Sinitskii, Nat. Commun. **5**, 3189 (2014).
[15] D. V. Kosynkin, A. L. Higginbotham, A. Sinitskii, J. R. Lomeda, A. Dimiev, B. K. Price, and J. M. Tour, Nature (London) **458**, 872 (2009).
[16] A. Chuvilin, E. Bichoutskaia, M. C. Gimenez-Lopez, T. W. Chamberlain, G. A. Rance, N. Kuganathan, J. Biskupek, U. Kaiser, and A. N. Khlobystov, Nat. Mater. **10**, 687 (2011).
[17] J. Cai, P. Ruffieux, R. Jaafar, M. Bieri, T. Braun, S. Blankenburg, M. Muoth, A. P. Seitsonen, M. Saleh, X. Feng, K. Müllen, and R. Fasel, Nature (London) **466**, 470 (2010).
[18] Y.-T. Lin, H.-C. Chung, P.-H. Yang, S.-Y. Lin, and M.-F. Lin, Phys. Chem. Chem. Phys. **17**, 16545 (2015).

[19] X. Wang, X. Li, L. Zhang, Y. Yoon, P. K. Weber, H. Wang, J. Guo, and H. Dai, Science **324**, 768 (2009).
[20] S. Yu, W. Zheng, Q. Wen, and Q. Jiang, Carbon N. Y. **46**, 537 (2008).
[21] B. Huang, Q. Yan, G. Zhou, J. Wu, B.-L. Gu, W. Duan, and F. Liu, Appl. Phys. Lett. **91**, 253122 (2007).
[22] J. Jiang, J. Turnbull, W. Lu, P. Boguslawski, and J. Bernholc, J. Chem. Phys. **136**, 014702 (2012).
[23] I.-Y. Jeon, H.-J. Choi, M. J. Ju, I. T. Choi, K. Lim, J. Ko, H. K. Kim, J. C. Kim, J.-J. Lee, D. Shin, S.-M. Jung, J.-M. Seo, M.-J. Kim, N. Park, L. Dai, and J.-B. Baek, Sci. Rep. **3**, 2260 (2013).
[24] Q. Miao, L. Wang, Z. Liu, B. Wei, F. Xu, and W. Fei, Sci. Rep. **6**, 21832 (2016).
[25] C. P. Ewels, D. Erbahar, P. Wagner, X. Rocquefelte, R. Arenal, P. Pochet, M. Rayson, M. Scardamaglia, C. Bittencourt, and P. Briddon, Faraday Discuss. **173**, 215 (2014).
[26] G. Kresse and J. Hafner, Phys. Rev. B **47**, 558 (1993).
[27] G. Kresse and J. Hafner, Phys. Rev. B **49**, 14251 (1994).
[28] G. Kresse and J. Furthmüller, Comput. Mater. Sci. **6**, 15 (1996).
[29] G. Kresse and J. Furthmüller, Phys. Rev. B **54**, 11169 (1996).
[30] J. P. Perdew, K. Burke, and M. Ernzerhof, Phys. Rev. Lett. **77**, 3865 (1996).
[31] J. P. Perdew, K. Burke, and M. Ernzerhof, Phys. Rev. Lett. **78**, 1396 (1997).
[32] M. Parrinello and A. Rahman, Phys. Rev. Lett. **45**, 1196 (1980).
[33] M. Parrinello and A. Rahman, J. Appl. Phys. **52**, 7182 (1981).
[34] S. Jun, X. Li, F. Meng, and C. V. Ciobanu, Phys. Rev. B **83**, 153407 (2011).
[35] T. Wassmann, A. P. Seitsonen, A. M. Saitta, M. Lazzeri, and F. Mauri, Phys. Rev. Lett. **101**, 096402 (2008).
[36] A typical error in binding energy for molecule is 30 kcal/mol. D. Rappoport, N. R. M. Crawford, F. Furche, and K. Burke, "Approximate density functionals: Which should i choose?" in *Encyclopedia of Inorganic Chemistry* (John Wiley & Sons, Ltd, Chichester, England, 2006).
[37] B. Huang, M. Liu, N. Su, J. Wu, W. Duan, B.-l. Gu, and F. Liu, Phys. Rev. Lett. **102**, 166404 (2009).
[38] Y.-W. Son, M. L. Cohen, and S. G. Louie, Phys. Rev. Lett. **97**, 216803 (2006).
[39] H. Lee, Y.-W. Son, N. Park, S. Han, and J. Yu, Phys. Rev. B **72**, 174431 (2005).
[40] See Supplemental Material at http://link.aps.org/supplemental/10.1103/PhysRevB.97.235436 for the phonon spectra for all the systems.